MAGNETIC BEHAVIOR AND ANTIBACTERIAL ACTIVITY OF IRON (III) COMPLEXES

PIEDAD CORTÉS-CORTÉS[1], ANA MARÍA ATRIA[1]*, MARTÍN CONTRERAS[1],
OCTAVIO PEÑA[2], KATIA FERNÁNDEZ[3], GINO CORSINI[3]

[1]Facultad de Ciencias Químicas y Farmacéuticas, Universidad de Chile. Santiago, Chile.
[2]L.C.S.I.M./UMR 6511CNRS/Institut de Chimie de Rennes, Université de Rennes I. Rennes, Francia.
[3]Laboratorio de Bacteriología Molecular, Facultad de Ciencias de la Salud, Universidad Diego Portales. Santiago, Chile.
(Received: 5 June 2007 - Accepted: 12 March 2008)

ABSTRACT

The preparation, magnetic characterization and antimicrobial properties of the complexes [Fe$_3$O(CH$_3$COO)$_6$(CH$_3$COOH)(H$_2$O)]Cl(MeImid)·(H$_2$O) **(1)** and [Fe$_4$O$_2$(CH$_3$COO)$_7$O$_2$(BPA)$_2$(H$_2$O)]· Cl·1.25(CH$_3$CH$_2$OH)(H$_2$O) **(2)**, where MeImid is 2-methyl-imidazolium and BPA is 2,2´-bipyridine, are described.

The variable temperature susceptibilities of these complexes were investigated in the temperature range 2-300K. The data have been modeled on the assumption of "butterfly" arranged for **(2)** and equilateral triangle of ferric ions for **(1)**.

The antimicrobial activities of these complexes have been screened *in vitro* against different bacterial strains. The complexes **(1)** and **(2)** display activity over Gram negative bacteria and these compounds not present activity over Gram positive strains. These complexes have bacteriostatic effect over bacterial target. The toxicity analyses of iron complexes showed these have cytotoxicity effect to values around the MIC on human cell.

Keyword: iron complexes, magnetism, antibacterial activities.

INTRODUCTION

The transition metals play a wide variety of roles in biology. Some metals are essential for biological function and are found in enzymes and cofactors required for various processes. Transition metals also plays a role as drugs to treat of variety of diseases and conditions [1-3].

Particularly important in the biological system is the iron ion. For example *E. coli* devotes almost 50 genes to proteins involved in iron uptake, while the potential for mammalian tumors to develop can be estimated by the density of their transferrin receptors, which are required for iron uptake and therefore essential for cell growth [4].

From a biological point of view, oxo- and hydroxo-bridged diiron units are wide occurrence in biology and perform a range of activities such as oxygen transport [5] and hydroxylation of alkanes [6].

The $\{$Fe$_3$O$\}^{7+}$ units has been proposed as the smallest building block of the ferritin core [7,8], since it is know that hemerythrin, methane monooxygenase and ribonucleotide reductase have diiron active sites with μ-oxo and μ-carboxylate bridges [9,10]. The ferric core of ferritine, exhibits the phenomenon of super paramagnetism [11]. Related system are the iron oxo complexes, which contain Fe(III) ions disposed in a "Butterfly" [Fe$_4$O$_2$]$^{8+}$ [12,13].

As a contribution to the general understanding of oxo-bridged polynuclear iron complexes we present herein the preparation, magneto-structural characterization of two oxo-bridged iron(III) ionic complexes, *viz*. [Fe$_3$O (CH$_3$COO)$_6$(CH$_3$COOH)(H$_2$O)]Cl(MeImid)·(H$_2$O) **(1)** and [Fe$_4$O$_2$(CH$_3$COO)$_7$ O$_2$(BPA)$_2$(H$_2$O)]·Cl·1.25 (CH$_3$CH$_2$OH)(H$_2$O) **(2)**, where MeImid = 2-methyl-imidazolium and BPA is 2,2´-bipyridine. We also studied the antibacterial activity, the action mechanism and cytotoxic effect on human cell of these two new iron oxo complexes.

EXPERIMENTAL SECTION

Reagents

Sodium acetate (Aldrich), 2,2´-bipyridine (Aldrich), iron (III) chloride (Aldrich) were used without further purification. The solvent (Fluka p.a. absolute ethanol) was used as received.

Synthesis

The complexes were synthesized according to the reported procedure by McCusker, *et al* [14]. To an orange solution of FeCl$_3$·6H$_2$O (2.67 mmol) in ethanol (50 mL) was treated with sodium acetate (6.63 mmol) and the respective ligand (1.43 mmol). The resultant solution was stirred at room temperature for 10 min. An excess of KClO$_4$ was added to the reaction mixture, and the resulting solution was stirred over night at room temperature. In both case a fine red-brown solid was collect by filtration. The solid was recrystallized in EtOH/ Et$_2$O.

Elemental analysis (C,H,N) were performed on a Carlo–Erba EA 1108 Instrument.

For complex **(1)** Anal. Found: C:26.92, H:4.09, N:3.65; Calc: C:27.05, H:4.14 N:3.71 and for complex **(2)** Anal. Found: C:39.21, H:4.71, N:4.98;

Calc: C: 39.33, H: 4.75, N:5.03.

The chemical analyses of **(1)** and **(2)** were in agreement with the structures described in reference [15].

Magnetic susceptibility measurements.

The magnetic susceptibility data were determined for the power samples over the temperature range 2-300K by using a SQUID magnetometer (QUANTUM DESING MODEL MPMS-XL5 instrument) with a field of 0.1T.

All susceptibility data were corrected for the diamagnetism of constituent atoms using Pascal´s constant [16].

EPR spectra

EPR spectra were recorder in X band (9.85GHz) on a Bruker ECS 106 spectrometer using a rectangular cavity with a 50 KHz field modulation.

Antibacterial activity

Bacterial strains used in this study are property of the Molecular Bacteriology Laboratory collection (Universidad Diego Portales). *Staphylococcus aureus* AB68, *Bacillus cereus* UDP346, *Pseudomonas aeruginosa* SJD1 and *Salmonella enteritidis* UDP455 strains were isolated from clinical samples while the *Escherichia coli* ATCC25922 and *Klebsiella pneumoniae* ATCC13833 strains was obtained from American Type Culture Collection.

Bacteria were grown in Mueller Hinton agar (Difco) or Mueller Hinton broth (Difco) for 16 to 24 h at 37 ºC in an incubator. The antibacterial activity of the complexes was tested *in vitro* using the paper disk diffusion method [17]. The complexes under study were dissolved in absolute ethanol and added to sterile 6 mm diameter paper disk. The quantitative antibacterial activity was determined using the minimum inhibitory concentration method (MIC) [18].

Antibacterial mechanism

The antibacterial effect of the complexes was tested *in vitro* using the chromogenic plate test assay [19]. *E. coli* BL21(DE3) which contains a chromosomal IPTG-inducible β-galactosidase gene, was used for the assays. First, an inoculum of this strain was grown overnight in 2 mL of Mueller Hinton medium, at 37 ºC with shaking. Then, a soft agar incubation mix containing 5 mL of 0.8% agar previously melted at 45 ºC, 0.1 mL of the bacterial cell inoculum, 0.01 mL of 1 mM IPTG, and 0.1 mL of 50 mg/mL X-Gal was vortex mixed and carefully overlaid on Mueller Hinton agar plates prepared the day before. Once soft agar was solidified and dried (1-2 h), a disk containing 400 µg of iron complexes or ampicillin was deposited on the soft agar layer. The plates were incubated at 37 ºC for 12-24 h. After incubation, inhibition zones were visually inspected by color formation along the edge of the disks and the plates were photographed. Only compounds causing cellular lysis produce a blue-colored edge at the inhibition zone.

Cytotoxic effect

The cytotoxicity of the iron complexes was tested *in vitro* on human kidney

embryonic cells (HEK293 cells) grown in microplates with DMEM medium plus 10% bovine fetal serum. After 24 h incubation with the iron complexes, the number of dead cells was determined with a vital dye trypan blue assay [20].

RESULTS AND DISCUSSION

Structure Descriptions

Both structures $[Fe_3O(CH_3COO)_6(CH_3COOH)(H_2O)]Cl(MeImid)\cdot(H_2O)$ **(1)** and $[Fe_4O_2(CH_3COO)_7O_2(BPA)_2(H_2O)]\cdot Cl\cdot 1.25(CH_3CH_2OH)(H_2O)$ **(2)** can be described in general terms as formed by isolated cationic clusters composed of Fe^{3+} ions coordinated to oxo and acetate anions.

The complex **(1)** consists in the triangular ensemble of three Fe(III) ions with the center oxo bridge which is stabilized by seven acetate ligands and two water molecules (Figure 1). Each iron atoms exhibit a distorted octahedral FeO_6 coordination environment. The complex **(2)** comprised an innermost core of two iron atoms doubly bridged by oxygen atoms, the oxo units, which in turn connect outward to the remaining iron atoms (one each), the second and third iron atom, to fulfill their μ_3- coordination (Figure 2).

These clusters, in turn, are stabilized by external anionic groups formed by a central chloride ion surrounded by different solvates to which the anion is tightly bound through H-bonding. Figures 1 and 2 present views of both structures. The detailed discussion of the X-ray structure, data collection, structure solution, and refinement of these complexes can be found in reference [15].

Figure 2. Close view of the tetrameric core in **(2)**, with hydrogen and (some) carbon atoms removed, for clarity. In double dashed lines, the intramolecular H-bond connecting O1W and acetato 9.

Magnetic susceptibility studies

The study of magnetic properties of the compounds **(1)** and **(2)** were performed through magnetic susceptibility measurements, on polycrystalline samples in the temperature range 5-300K in 0.1T field.

For the complex $[Fe_3O(CH_3COO)_6(CH_3COOH)(H_2O)]Cl(MeImid)\cdot(H_2O)$ **(1)** the temperature dependences of their magnetic susceptibilities were plotted in Figure 3, in the form of χ_M^{-1} *vs* T and $\chi_M T$ *vs* T.

The inverse of the molar magnetic susceptibility decreases with decreasing temperature over the whole range.

The $\chi_M T$ versus T plot shows that the $\chi_M T$ product gradually decreases from 3.43 $cm^3\ mol^{-1}K$ at 300K to 0.825 $cm^3\ mol^{-1}K$ at 6K. The observed effective magnetic moment per molecule at 6K is 2.56MB, while at room temperature it is 5.23MB. This last value is smaller than expected for three non interacting iron(III) ions. The data are suggestive of a coupling occurs between the ferric ions.

In light of the structure of **(1)**, the system was assumed to consist of three identical metal ions which arranged at the corner of an equilateral triangle, producing three equal interactions. The magnetic interactions can be illustrated by means of scheme 1

Figure 1. Close view of the trimeric core in **(1)**, with hydrogen and (some) carbon atoms removed, for clarity.

$$\chi = \frac{Ng^2\beta^2}{12kT}\left(\frac{340+455e^{15x}+429e^{28x}+330e^{39x}+210e^{48x}+105e^{55x}+20e^{60x}+e^{63x}}{4+7e^{15x}+9e^{28x}+10e^{48x}+9e^{55x}+4e^{60x}+e^{63x}}\right)$$

Equation 1

where x= exp(J/kT) and χ_M , k parameters in equation 1 have their usual meanings.

The magnetic susceptibility expression was fitted to the experimental magnetic data by using a non linear least–squares fitting by minimizing the function R= $\Sigma[(\chi_M)_{obs}-(\chi_M)_{cal}]^2/\Sigma[(\chi_M)_{obs}]^2$.

A g-value of 1.9 was obtained from EPR spectra and used as a constant in the least-squares fitting process. The best fitting parameter obtained for **(1)** is J=-2.71cm^{-1} with R= 8.79x10^{-4}. The solid line in the Figure 4 was calculated with this parameter. The results of the fit are indicative of weak antiferromagnetic exchange within the cluster.

Figure 4. Thermal dependence of χ_M for [Fe$_3$O(CH$_3$COO)$_6$(CH$_3$COOH)(H$_2$O)]·Cl(MeImid)·(H$_2$O) **(1).** The solid line represents the best fit of the experimental data.

The crystal structure of an iron (III) complex of this type, is the compound [Fe$_3$O(TIEO)$_2$(O$_2$CPh)$_2$Cl$_3$] **(3)** reported by Lippard *et al.*, where the ligand TIEOH is the 1,1,2-tris(N-methylimidazol-2-yl)-3-hidroxyethane, and O$_2$CPh is benzoate [21].

Comparison of the structure reported here complex **(2)** with that of, complex **(3)** indicates that both structures are similar. We note that in both cases the Fe atoms placed in the triangular array. In the complex **(3)** the Fe-Fe distances are Fe(1)-Fe(3) =3.018(1) Å , Fe(2)-Fe(3) = 3.027(3) Å, Fe(1)-Fe(2) = 3.667(1)Å. This three iron atoms defined an isosceles triangle. The Fe-O-Fe angles are Fe(1)-O(3)-Fe(2)= 159.1(3)°, Fe(1)-O(3)-Fe(3)=100.3(3)°and Fe(2)-O(3)-Fe(3)=100.5(3)°. Each iron atom has pseudooctahedral symmetry, with two nitrogen, three oxygen and one chlorine atom in the coordination spheres of the equivalent Fe1 and Fe2 atoms. Five oxygen and one chlorine atom constitute the coordination sphere of the unique Fe3 atom.

The exchange interaction in this Fe$_3$-trimer, complex **(3)**, is discusses in terms of the isosceles triangular array of metal atoms. The analysis yielded J$_{12}$= -55cm^{-1} and J$_{13}$=J$_{23}$= -8.0 cm^{-1}, with the large antiferromagnetic coupling interaction occurring between iron centers linked by the short μ-oxo bridge bonds.

In the complex **(1)** Fe$_3$O(CH$_3$COO)$_6$(CH$_3$COOH)(H$_2$O)]·Cl(MeImid)·(H$_2$O) the Fe$_3$O core is much more symmetric than the complex **(3)**. The average value distances Fe-Fe is 3.313Å, defining an equilateral triangle. The coordination spheres of the atoms of iron are constituted, in this case, by only oxygen atoms. The Fe-O1-Fe angle of the bridge are extremely close to 120º (Fe$_1$-O$_1$-Fe$_2$= Fe$_{1A}$-O$_1$-Fe$_2$=119.5(3); Fe$_1$-O$_1$-Fe$_2$=121.0(5), and the Fe-O$_{oxo}$ distances are Fe(1)-O(1)= 1.894Å ; Fe(2)-O(1)=1.950Å and Fe(1A)-O(1)=1.894 Å.

The magnetic properties on the title complex differ greatly in relation to complex (**3**), in this case the exchange constant is J= -2,71cm^{-1}.

The difference in the magnitude of exchange coupling must be associate to smaller number of the bridged acetate ligands between the metal ions.

For the complex [Fe$_4$O$_2$(CH$_3$COO)$_7$(H$_2$O)(BPA)$_2$]Cl·(CH$_3$CH$_2$OH)$_2$·

Figure 3. Plot of the temperature dependence of χ_M^{-1} and χ_MT for [Fe$_3$O(CH$_3$COO)$_6$(CH$_3$COOH)(H$_2$O)]· Cl(MeImid)·(H$_2$O) **(1)**

Scheme 1

The appropriate spin Hamiltonian to treat this problem is $H = -2J[(S_1 \cdot S_2)+(S_2 \cdot S_3)+(S_1 \cdot S_3)]$ where, J is the exchange coupling constant between the pair of iron (III) ion. S_1, S_2 and S_3 are the spin operator associated with the local spin S_1=S_2=S_3= $^5/_2$.

The magnetic susceptibility expression is giving as

(H_2O) **(2)** the inverse susceptibility and $\chi_M T$ product are plotted as a function of temperature in the Figure 5 The graph of reciprocal molar susceptibilities versus temperature not follow the Curie law.
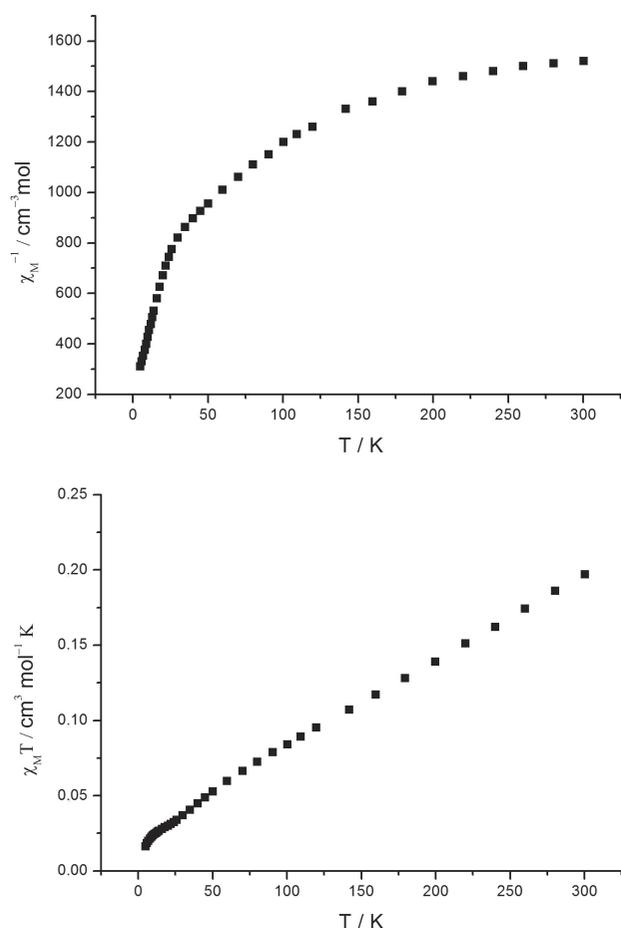
Figure 5. Plot of the temperature dependence of χ_M^{-1} and $\chi_M T$ for $[Fe_4O_2(CH_3COO)_7(H_2O)(BPA)_2]Cl\cdot(CH_3CH_2OH)_2\cdot(H_2O)$ **(2).**

The $\chi_M T$ product monotonically decreases from 0.197 cm³ mol⁻¹ K at 300 to 0.0162 cm³ mol⁻¹ K at 5K, the calculated magnetic moments per molecule are 1.26BM and 0.36BM respectively. The value of magnetic moment (1.26BM) is smaller than expected for four non interacting metallic centers with S=⁵/₂. This is indicative of the antiferromagnetic interactions within the cluster.

In the core Fe_4O_2 , the distances Fe_1-Fe_2, Fe_1-Fe_3, Fe_2-Fe_4 and Fe_3-Fe_4 are equals and Fe_1-Fe_4 is large, this suggest the pairwise magnetic exchange interactions between pairs Fe(III)-Fe(III) ions are equivalent such as $J_{12} = J_{13} = J_{24} = J_{34} = J_a$, and the coupling between the Fe_1-Fe_4 is different and equal to J_b.

The spin Hamiltonian describing the isotropic exchange interaction for a tetranuclear "butterfly" arrangement of metal ions is giving by equation 2 and the scheme 2 shows the magnetic model used in the analysis of the susceptibilities for this complex, which include two different J values.

$$H= -2J_a (S_1\cdot S_2 + S_1\cdot S_3 + S_3\cdot S_4 + S_4\cdot S_2) -2J_b (S_1\cdot S_4), \quad \text{Equation 2}$$
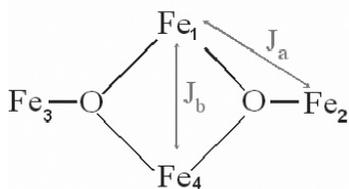
Scheme 2

The expression for the molar paramagnetic susceptibility, χ_M derived by using the Van Vleck equation[14] .The solid line in the Figure 6 represent the result obtained from fitting to the experimental data using a least-square fitting routine with the EPR determined g value of 1.9 as a constant parameter. The best fit was found with J_a= -16.20 cm⁻¹ and J_b= -9.78 cm⁻¹, with R= 6.22×10^{-3} (R= $\Sigma[(\chi_M)_{obs}-(\chi_M)_{cal}]^2/\Sigma[(\chi_M)_{obs}]^2$) .
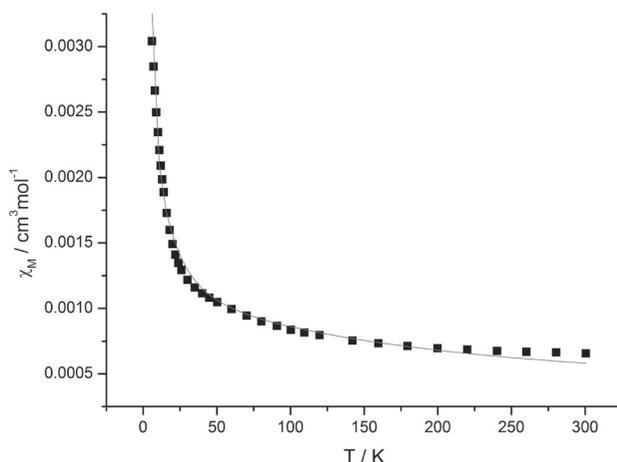
Figure 6. Thermal dependence of χ_M for $[Fe_4O_2(CH_3COO)_7(H_2O)(BPA)_2]$ Cl· $(CH_3CH_2OH)_2$· (H_2O) **(2).** The solid line represents the best fit of the experimental data.

These values are indicative of antiferromagnetic interaction between iron centers.

An examination of the Table 1, in which the magnetic properties of other complexes of this kind are tabulated reveals that, J_b constant is much less than J_a constant. The difference in the magnitude of the interactions, $e.g.\,J_a$ interaction greater than J_b can be associated to spin frustration in these systems. The strength of the J_a interaction relative to J_b interaction is such that the natural tendency for the spin vectors on Fe(1) and Fe(4) to align antiparallel is overcome and the result is an ferromagnetic alignment of Fe(1) Fe (4) spin vectors and frustration of that spin spin interaction .

Table 1. Comparative magnetic data for Fe_4O_2 complexes.

Compounds	J_a/cm⁻¹	J_b/cm⁻¹	
$[Fe_4O_2(O_2CCH_3)_7(bpy)_2]^+$	-91.0	-17.8	Ref. 14
$[Fe_4O_2(O_2CPh)_7(phen)_2]^+$	-77.6	-2.4	Ref. 13
$[Fe_4O_2(O_2CPh)_8(phen)_2]$	-65.7	-15.6	Ref. 13
$[Fe_4O_2(CH_3COO)_7(BPA)_2(H_2O)]^+$	-16.2	-9.8	This work

Antibacterial activity and cytotoxicity

Table 2 shows the antimicrobial effect of compound using the paper disk diffusion method. From the zone of bacterial grown inhibition, it is observed that all the complexes showed activity towards Gram negative bacteria analysed. In the other hand, against Gram positive bacteria we did not find any activity for the complex **(1)** and we find minimal activity for the complex **(2)** against *Staphylococcus aureus*. These results showed that both iron complexes synthesized in this work have not present significant activity over Gram positive strains.

The analysis of minimum inhibitory concentration included in table 3 showed that both complexes have MIC values slightly higher than ampicillin under conditions studied (with MIC values around 60-70 μg/mL).

We used a plate assay to distinguish a bacteriolytic from a bacteriostatic mode of action of antimicrobial complexes [19]. This method is based on the use of β-galactosidase as an appropriate marker of cellular lysis. If lysis occurs, then the enzyme is released outside the bacterium and detected on the plate. When the enzyme reaches the agar medium, it hydrolyzes the 5-bromo-4-chloro-3-indolyl-β-D-galactoside (X-Gal), a chromogenic compound included in the agar. After overnight incubation, X-Gal forms a blue circle staining the edge of the inhibition zone produced by the antibiotic application. Only compounds causing cellular lysis produce a blue-colored edge at the inhibition zone.

Table 2. Qualitative antibacterial activity of iron (III) complexes

Bacteria	Zone of inhibition (mm)*			
	Fe/2MeIm (1)	Fe/BPA (2)	Ampicillin	Solvent** (etanol)
Gram positive				
Staphylococcus aureus AB68	R	9	29	R
Bacillus cereus UDP356	R	R	R	R
Gram negative				
Eschericia coli ATCC25922	18	17	24	R
Klebsiella pneumoniae ATCC13833	15	15	23	R

 * Used disk with 400 μg iron complexes and 400 μg ampicillin. Number of assays = 3, estimated error ± 1 mm. R is resistant
 ** The solvent was added to paper disk over equals conditions to disk with iron complexes.

Table 3. Quantitative Antibacterial activity of iron (III) complexes.

Bacteria	MIC (μg/mL)*		
	Fe/2MeIm (1)	Fe/BPA (2)	Ampicillin
Eschericia coli ATCC25922	75	70	62.5
Klebsiella pneumoniae ATCC 13833	55	70	62.5
Salmonella enteritidis UDP455	65	70	125
Pseudomonas aeruginosa SJD1	55	50	>1000

 * Number of assays = 3, R is resistant.

The assay showed that both iron complexes present bacteriostatic activity because they do not produce a blue circle staining the edge of the inhibition zone (Figure 7). As controls, we used chloramphenicol and ampicillin as bacteriostatic and bacteriolytic agents, respectively.

The toxicity of iron complexes was tested on human kidney cells (Figure 8). The values of IC_{50} for **(1)** and **(2)** were 84.3 and 48.5 μM, respectively. It could be observed that complexes presented significant cytotoxicity effect at values around the MIC (70 μM and 60 μM for **(1)** and **(2)** respectively). On the other hand, these complexes have not shown toxic effects at values one or two magnitude order less than the MIC.
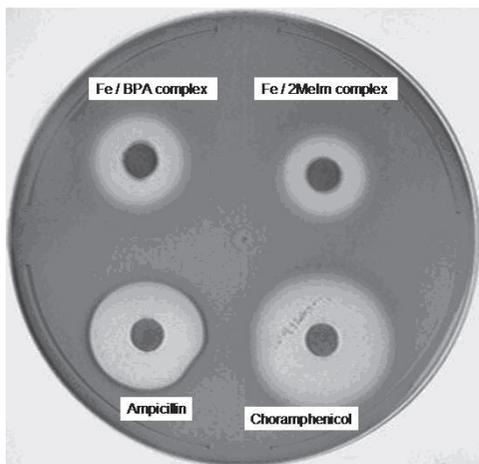
Figure 7. Plate assay showing bacteriostatic activity for the iron complexes. Ampicillin is a bacteriolytic control and chloramphenicol is a bacteriostatic control.
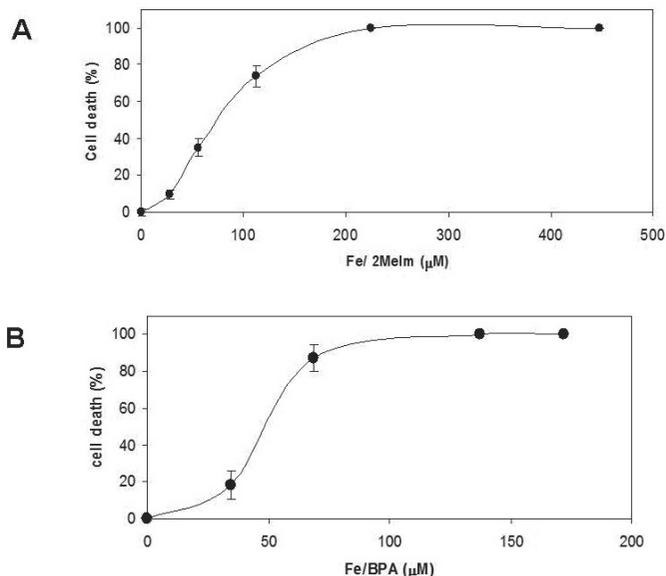
Figure 8. The Cytotoxicity effect over human cell of $[Fe_3O(CH_3COO)_6(CH_3COOH)(H_2O)]Cl$ (MeImid)·(H_2O) **(1)** (Plot A) and $[Fe_4(CH_3COO)_7O_2(BPA)_2(H_2O)]\cdot Cl\cdot 1.25(CH_3CH_2OH)(H_2O)$ **(2)** (plot B) complexes.

CONCLUSIONS

A trimeric and tetrameric Fe(III) complexes have been synthesized, and characterized by magnetic measurements. The magnetic data of **(1)** and **(2)** show that the coupling between Fe(III)-Fe(III) are antiferromagnetic in nature. These data are in qualitative agreement with complexes previously reported, although the intensity of the coupling is lower in this case.

Although these complexes have antibacterial activity through a bacteriostatic mechanism, they are cytotoxic to human cells. However, they could possibly be used as disinfectants since after being applied to a surface and later washed away, the toxicity would be very low since the remaining amounts are 10 to 100-fold smaller than the MIC and the cell survival is between 95 to 99 %.

ACKNOWLEDGMENT

REFERENCES

1. M. S Islam, M.A. Farooque, M.A.K.Bodruddoza, M.A. Mosaddik, M.S. Alam. *J. Biol. Sci. 2*, 797, (2002).
2. P.Cortés, A.M. Atria, M.T.Garland, R.Baggio, O. Peña, G. Corsini. *J. Chil.Chem. Soc.* **51**,843, (2006).
3. P.Cortés, A.M. Atria, M. Contreras, M.T.Garland, O. Peña, G.Corsini. *J. Chil. Chem. Soc.* **51**, 961, (2006).
4. R.R.Crichton . Inorganic Biochemistry of Iron Metabolism from Molecular Mechanisms to Clinical Consequences. John Wiley and Sons, Chichester and New York, 2001.
5. M.A. Holmes, R.E.Stenkamp, *J. Biol. Mol.* **220**, 773,(1991).
6. A.C.Rosenzweig, C.A. Frederick, S.J.Lippard, P. Nordlund. *Nature.* **366**, 537, (1993).
7. M.E.Holt, S.L. Holt, W.F. Tucker, N.D. Asplund, K.J. Watson. *J. Am. Chem. Soc.* **96**, 2621, **(**1974).
8. S.M.Heald, E.A. Stearn, B. Bunker,E.Holt, S.L. Holt. *J. Am. Soc.* **101**, 67, (1979)**.**
9. P.C.Wilkins, R.G.Wilkins. *Coord. Chem. Rev.* **79**, 195, **(**1987).
10. A.Ericson, B. Hedman, K.O. Hodgson, J. Green, H.Dalton, J.G. Bentsen, R.H. Beer, S.J. Lippard. *J. Am. Chem. Soc.* **110**, 2330, (1988).
11. E.C.Theil. *Annu. Rev. Biochem.* **56**, 289, (1987).
12. A.K.Boudalis,V. Tangoulis, C.P.Raptopoulou, A. Terzis, J.P. Tuchagues, S.P. Perlepes. *Inorg. Chim. Acta.* **357**, 1345, (2004)**.**

13. A.K.Boudalis, N.Lalioti, G.A. Spyroulias, C.P. Raptopoulou, A. Terzis, A.Bousseksou, V. Tangoulis, J.P.Tuchagues, S.P. Perlepes. *Inorg.Chem.* **41**, 6474, (2002).

14. J.K.McCusker, J.B.Vincent, E.A.Schmitt, M.L. Mino, K. Shin, D.K. Coggin, P.M.Hagen, J. C.Huffman, G. Christou, D.N. Hendrickson. *J. Am. Chem. Soc.* **113**, 3012, (1991).

15. P.Cortés, A.M. Atria, M.T. Garland, R. Baggio. *Acta Cryst. C* **62**, m297,(2006).

16. A.Earnshaw. Introduction to Magnetochemistry. Academic Press; London, 1968.

17. K.L.Waniewska. *Bull. Environ. Contam.Toxicol.* **27**, 289, (1981).

18. National Committee for Clinical Laboratory Standards. Methods for Dilution Antimicrobial Susceptibility Tests for Bacteria That Grow Aerobically-Fifth Edition: Approved Standard M7-A5; NCCLS, Wayne, PA, USA. 2000.

19. G.Mardones, A. Venegas. *J. Microbiol. Meth.,* **40**, 199, (2000).

20. R.Freshey. Culture of animal cells: a manual of basic technique; Alan R. Liss Inc., New York, p117, 1987.

21. S.M.Gorun, G.C. Papaefthymiou, R.B. Frankel, S.J. Lippard. *J. Am. Chem. Soc.* **109***, 4244. (1987).